

# Electron Transport in Nanogranular Ferromagnets

I. S. Beloborodov,<sup>1,2</sup> A. Glatz,<sup>1</sup> and V. M. Vinokur<sup>1</sup>

<sup>1</sup>Materials Science Division, Argonne National Laboratory, Argonne, Illinois 60439, USA

<sup>2</sup>James Franck Institute, University of Chicago, Chicago, Illinois 60637, USA

(Dated: February 1, 2008)

We study electronic transport properties of ferromagnetic nanoparticle arrays and nanodomain materials near the Curie temperature in the limit of weak coupling between the grains. We calculate the conductivity in the Ohmic and non-Ohmic regimes and estimate the magnetoresistance jump in the resistivity at the transition temperature. The results are applicable for many emerging materials, including artificially self-assembled nanoparticle arrays and a certain class of manganites, where localization effects within the clusters can be neglected.

PACS numbers: 71.10.-w, 75.10.-b, 73.43.Qt

Arrays of ferromagnetic nanoparticles are becoming one of the mainstreams of current mesoscopic physics [1, 2, 3, 4]. Not only ferromagnetic granules promise to serve as logical units and memory storage elements meeting elevated needs of emerging technologies, but also offer an exemplary model system for investigation of disordered magnets. At the same time the model of weakly coupled nanoscale ferromagnetic grains proved to be useful for understanding the transport properties of doped manganite systems [5, 6] that have intrinsic inhomogeneities. Recent studies showed that above the Curie temperature these materials possess a nanoscale ferromagnetic cluster structure which to a large extent controls transport in these systems [7, 8, 9, 10]. This defines an urgent quest for understanding and quantitative description of electronic transport in ferromagnetic nanodomain materials based on the model of nanogranular ferromagnets.

In this paper we investigate electronic transport properties of arrays of ferromagnetic grains [11] near the ferromagnetic-paramagnetic transition, see Fig. 1. At low temperatures,  $T < T_c^s$ , the sample is in a so called *superferromagnetic* (SFM) state, see Fig. 1, set up by dipole-dipole interactions. Near the *macroscopic* Curie temperature,  $T_c^s$ , thermal fluctuations destroy the macroscopic ferromagnetic order. At intermediate temperatures  $T_c^s < T < T_c^g$ , where  $T_c^g$  is the Curie temperature of a single grain, the system is in a *superparamagnetic* (SPM) state where each grain has its own magnetic moment while the global ferromagnetic order is absent. At even higher temperatures,  $T > T_c^g$ , the ferromagnetic state within each grain is destroyed and the complete sample is in a paramagnetic state. We consider the model of weakly interacting grains in which the sample Curie temperature is much smaller than the Curie temperature of a single grain,  $T_c^s \ll T_c^g$ .

We first focus on the SPM state, and discuss a  $d$ -dimensional array ( $d = 3, 2$ ) of ferromagnetic grains taking into account Coulomb interactions between electrons. Granularity introduces additional energy parameters apart from the two Curie temperatures,  $T_c^g$  and  $T_c^s$ : each nanoscale cluster is characterized by (i) the charging

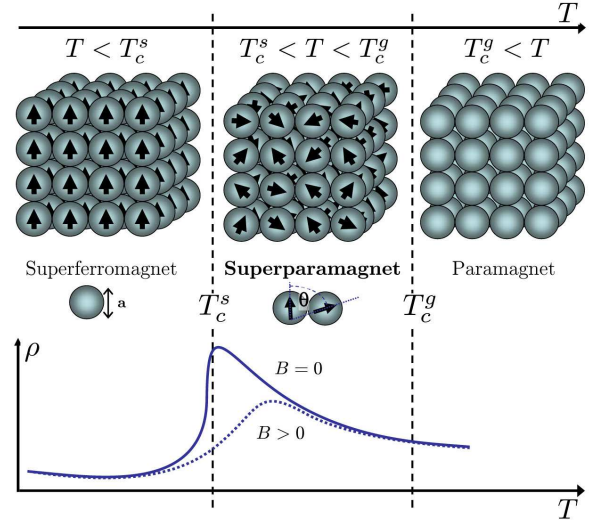


FIG. 1: Top: Sketch of a 3d granular system under consideration showing the different states at different temperatures: For  $T < T_c^s$ , where  $T_c^s$  is the macroscopic Curie temperature of the system, the ferromagnetic grains (*superspins*) form a superferromagnet (SFM); for  $T_c^s < T < T_c^g$ , where  $T_c^g$  is the Curie temperature for a single grain, the system is in a superparamagnetic (SPM) state; and above  $T_c^g$  the system shows no magnetic order. In the SPM state the angle between two grains (superspins) is denoted by  $\theta$ . Note, this is an idealized picture, see [11]. Bottom: Schematic behavior of the resistivity,  $\rho$ , versus temperature,  $T$ , in the different states in the absence ( $B = 0$ ) and presence ( $B > 0$ ) of a magnetic field  $B$  aligned with the magnetization of the SFM, cf. [3, 12].

energy  $E_c = e^2/(\kappa a)$ , where  $e$  is the electron charge,  $\kappa$  the sample dielectric constant, and  $a$  the granule size, and (ii) the mean energy level spacing  $\delta$ . The charging energy associated with nanoscale ferromagnetic grains can be as large as several hundred Kelvins [11] and we require that  $E_c/\delta \gg 1$ . The typical sample Curie temperature,  $T_c^s$ , of the arrays we consider (and also of doped manganites) is in the range  $(100 - 200)K$ , [3, 12, 13]; thus the temperature interval  $T_c^s < T < E_c$  is experimentally accessible. To satisfy the last inequality, the size of a single ferromagnetic grain,  $a$ , should be less than the critical size  $a_c = e^2/(T_c^s \kappa)$ . The condition  $E_c/\delta \gg 1$  defines the

lower limit for the grain size:  $a_l = (\kappa/e^2\nu)^{1/(D-1)}$ , where  $\nu = \nu_\uparrow + \nu_\downarrow$  is the total density of states at the Fermi surface (DOS) with  $\nu_{\uparrow(\downarrow)}$  being the DOS for electrons with spin up (down) and  $D$  the grain dimensionality [14].

The internal conductance of a metallic grain is taken much larger than the inter-grain tunneling conductance, which is a standard condition of granularity. The tunneling conductance is the main parameter that controls macroscopic transport properties of the sample [15]. In consideration of applications to experiments [1, 3, 13, 16] we restrict ourselves to the case where the tunneling conductance is smaller than the quantum conductance [17]. In the SPM state the charge degrees are coupled with the spin degrees of freedom; to reflect this connection, the tunneling conductance can be written in a form  $\tilde{g}_t(\theta) = g_t^0(1 + \Pi^2 \cos \theta)$ , [18], where  $g_t^0$  is the tunneling conductance in the paramagnetic state [19];  $\Pi = (\nu_\uparrow - \nu_\downarrow)/(\nu_\uparrow + \nu_\downarrow)$  is the polarization factor of a ferromagnetic grain where  $\theta \in [0, \pi]$  is the angle between two superspins, see Fig. 1. The tunneling conductance,  $\tilde{g}_t(\theta)$ , achieves its maximum value for parallel spins,  $\theta = 0$  (corresponding to the SFM state). In general, the distribution of angles  $\theta$  is determined by some function  $f(\theta)$  which depends on temperature (and on external magnetic field): for  $T < T_c^s$ , in the SFM state  $f(\theta)$  is the  $\delta$ -distribution and for high temperatures,  $T \gg T_c^s$ , it is constant [an explicit expression for  $f(\theta)$  is discussed below Eq. (3)]. We denote averages over angles by  $\langle \dots \rangle_\theta \equiv \int_0^\pi d\theta \dots f(\theta)$  with  $\langle 1 \rangle_\theta = 1$ . Using this distribution we introduce the averaged tunneling conductance:

$$g_t(m^2) \equiv \langle \tilde{g}_t(\theta) \rangle_\theta = g_t^0(1 + \Pi^2 m^2), \quad (1)$$

with the normalized "magnetization"  $m^2 = \langle \cos \theta \rangle_\theta$ , e.g.  $m^2 = 1$  in the SFM state and  $m^2 \rightarrow 0$  for high temperatures,  $T \gg T_c^s$ . Note, that in general  $m^2$  is not the normalized (absolute value of the) magnetization of the sample since it only takes into account the angle between two neighboring superspins in the plane spanned by them (Fig. 1). However, close to  $T_c^s$ , we can expect  $m^2 \approx |\mathbf{M}(T)/M_s|^2$ , where  $M_s$  is the saturation value of the magnetization of the sample. Below we first discuss the Ohmic transport near  $T_c^s$  and then summarize the main results for the resistivity behavior in the non-Ohmic regime.

*Ohmic transport.*— To calculate the conductivity for weakly coupled grains in the presence of quenched disorder, we start with determining the total probability for an electron to tunnel through  $N$  grains  $\tilde{P}(\theta_1, \dots, \theta_N) = \prod_{i=1}^N \tilde{P}_i(\theta_i)$ , where  $\tilde{P}_i(\theta_i)$  denotes the probability for an electron to tunnel through a single grain  $i$  with an angle difference  $\theta_i$  of the magnetic moment to the previous grain [15, 20]. The probability  $\tilde{P}(\theta_1, \dots, \theta_N)$  has to be averaged over all angles in order to obtain the total tunneling probability  $\mathcal{P}_{\text{total}} \equiv \langle \tilde{P}(\theta_1, \dots, \theta_N) \rangle_{\theta_1, \dots, \theta_N} = \prod_{i=1}^N \mathcal{P}_i(m^2)$ . The latter equality follows from the fact that  $\mathcal{P}_{\text{total}}$  factorizes

into the individually averaged probabilities  $\mathcal{P}_i(m^2) = \langle \tilde{P}_i(\theta_i) \rangle_{\theta_i}$ , [20]. The mechanism for electron propagation through an array of grains at low temperatures is elastic and/or inelastic co-tunneling. The corresponding probabilities in the limit of weak coupling between the grains [17] are given by  $\mathcal{P}_i^{\text{el}}(m^2) \simeq [g_t(m^2)\delta]/E_c$  and  $\mathcal{P}_i^{\text{in}}(m^2) \simeq [g_t(m^2)T^2]/E_c^2$ , respectively, [21]. Assuming that all probabilities  $\mathcal{P}_i(m^2)$  are approximately the same [11] for each grain,  $\mathcal{P}_i(m^2) = \mathcal{P}(m^2)$  for all  $i$ , and expressing them in terms of the localization length  $\xi(m^2)$ , defined by  $\mathcal{P}(m^2) = \exp[-a/\xi(m^2)]$ , we obtain [15]

$$\xi^{\text{el}} \simeq a/\ln[E_c/g_t(m^2)\delta], \quad \xi^{\text{in}} \simeq a/\ln[E_c^2/T^2 g_t(m^2)]. \quad (2)$$

Since the characteristic temperature we consider is of the order of the Curie temperature,  $T \sim T_c^s$ , the dominant mechanism for electron propagation is the inelastic co-tunneling [22]. Following Mott-Efros-Shklovskii's theory [23, 24], the conductivity can be written as  $\sigma(T, m^2) \sim g_t(m^2) \exp[-r/\xi(m^2) - e^2/(\kappa r T)]$ , where the tunneling conductance  $g_t(m^2)$  is given by Eq. (1) and  $r$  is the hopping distance. The first term in the exponent accounts for electron tunneling and the second term describes thermal activation necessary to overcome the Coulomb correlation energy. Optimizing  $\sigma(T, m^2)$  with respect to the hopping length,  $r = N \cdot a$ , we obtain:

$$\sigma(T, m^2) \sim g_t^0(1 + \Pi^2 m^2) \exp(-\sqrt{\mathcal{T}_0(m^2)/T}), \quad (3)$$

with  $\mathcal{T}_0(m^2) = T_0[1 - (\xi_0/a) \ln(1 + \Pi^2 m^2)]$  being the characteristic temperature scale. Here  $T_0 \equiv \mathcal{T}_0(m^2 = 0) = e^2/(\kappa \xi_0)$ , where  $\xi_0$  is the inelastic localization length given in Eq. (2) with the tunneling conductance corresponding to the paramagnetic state,  $g_t(m^2 = 0) = g_t^0$ . The minimal value of the resistivity in the SFM state is determined by the minimal value of the energy scale  $\mathcal{T}_0^{\text{min}} = T_0(1 - \ln 2)$ .

The behavior of the resistivity  $\rho(T, m^2)$ , inverse of the conductivity  $\sigma(T, m^2)$  in Eq. (3), and the magnetization  $m^2(T)$  are shown in Fig. 2 for the following set of parameters:  $\xi_0/a = 1$ ,  $T_0/T_c^s = 10$ , and  $\Pi^2 = 0.3$ . In order to describe typical experimental data [12], the normalized distribution function  $f(\theta)$  was chosen to ensure a sharp drop in the magnetization at  $T_c^s$ ,  $f[\alpha, x] = [\alpha/\arctan(1/\alpha)](x^2 + \alpha^2)^{-1}$ , with  $x = \theta/\pi$  and  $\alpha(T) = 10(T/T_c^s - 1)$  for  $T \geq T_c^s$  and  $\alpha(T < T_c^s) = 0$  otherwise. The numerical constant in  $\alpha(T)$  was taken to produce a drop of  $m^2$  in a temperature region  $\Delta T_c^s$  with  $\Delta T_c^s/T_c^s \sim 0.1$ . Note, that the jump in the resistivity does not depend on the precise functional expression of  $f(\theta)$ ; but it is sufficient that  $m^2$  decays rapidly in the interval  $\Delta T_c^s \ll T_c^s$ .

For small polarization factors,  $\Pi^2 m^2 \ll 1$ , the expression for the energy scale  $\mathcal{T}_0(m^2)$ , can be written as  $\mathcal{T}_0(m^2) = T_0[1 - (\xi_0/a)\Pi^2 m^2]$ . As a result, we obtain for the conductivity of an array of superspins  $\sigma(T, m^2) \sim [1 + \gamma_T \Pi^2 m^2] \exp(-\sqrt{\mathcal{T}_0/T})$ , where  $\gamma_T$  is

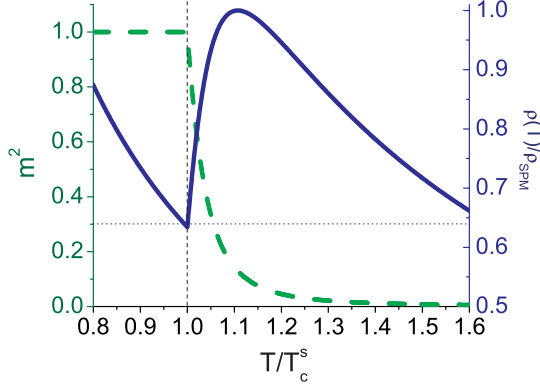


FIG. 2: Solid line, right axis: Plot of the normalized resistivity  $\rho(T, m^2)/\rho_{\text{SPM}}$ , inverse of the conductivity  $\sigma(T, m^2)$  in Eq. (3), vs. temperature for the following set of parameters:  $\xi_0/a = 1$ ,  $T_0/T_c^s = 10$ , and  $\Pi^2 = 0.3$ . Here  $\rho_{\text{SPM}} \equiv \rho(T_1, m_1^2)$  with  $T_1 > T_c^s$  being the temperature at which  $\rho(T, m^2)$  is maximal and  $m_1^2 \equiv m^2(T_1)$ . Dashed line, left axis: Plot of the "magnetization"  $m^2$  versus temperature using an angular distribution function defined in the text.

a temperature dependent function. For temperatures  $T_c^s \leq T \ll T_0$  it is given by  $\gamma_T \simeq (\xi_0/2a) \sqrt{T_0/T}$ . The last expression can be written in terms of the optimal hopping length,  $r_{\text{opt}} = \xi_0 \sqrt{T_0/T}$ , as  $\gamma_T \simeq r_{\text{opt}}/2a$ . Since the hopping length  $r_{\text{opt}}$  depends on temperature even within the SPM state, where the temperature  $T$  satisfies the inequality  $T_c^s < T < E_c$ , one expects to observe two different regimes: at temperatures  $T_c^s < T < T^*$  the dominant mechanism for electron propagation is variable range hopping [in this regime  $r_{\text{opt}} > a$ ], while for  $T^* < T < E_c$  electrons hop between the nearest neighbor grains only [ $r_{\text{opt}} \sim a$ ]. The separating temperature  $T^*$  can be estimated using the condition  $r_{\text{opt}} \simeq a$  which gives  $T^* \simeq T_0 (\xi_0/a)^2$ , i.e.  $T^* \leq T_0$ .

To calculate the magnitude of the jump value of the resistivity at the transition from the SPM to the SFM state in Fig. 2, we introduce the dimensionless resistance ratio  $\Delta\rho/\rho \equiv [\rho_{\text{SPM}} - \rho_{\text{SFM}}]/\rho_{\text{SPM}}$ , where  $\rho_{\text{SFM}}$  is calculated at temperature  $T = T_c^s$ , using the inverse of Eq. (3), for magnetization  $m^2 = 1$ ;  $\rho_{\text{SPM}}$  has to be evaluated at some temperature  $T_1 > T_c^s$  at which  $\rho(T, m^2)$  is maximal and magnetization  $m_1^2 \equiv m^2(T_1)$ . The temperature  $T_1$  is of the order of  $T_c^s + \Delta T_c^s$ ; but since the magnetization drops quickly above  $T_c^s$ , i.e.  $\Delta T_c^s \ll T_c^s$ , it is sufficient to take  $\rho_{\text{SPM}}$  at  $T_1 \sim T_c^s$  for calculating the jump. Using Eq. (3) we obtain the following result:

$$\frac{\Delta\rho}{\rho} \simeq 1 - \frac{1 + \Pi^2 m_1^2}{1 + \Pi^2} e^{-\sqrt{T_0(m_1^2)/T_c^s} + \sqrt{T_0(1)/T_c^s}}. \quad (4)$$

For small polarization factors,  $\Pi^2 \ll 1$ , this reduces to  $\Delta\rho/\rho \simeq (\xi_0/2a) \sqrt{T_0/T_c^s} \Pi^2 (1 - m_1^2)$ , and can be expressed in terms of  $r_{\text{opt}}$  as  $\Delta\rho/\rho \sim \Pi^2 r_{\text{opt}}(T_c^s)/a$ . Therefore the larger the hopping length, the bigger is the resistivity jump between the SPM and SFM states. From Eq. (4) follows that the resistance ratio  $\Delta\rho/\rho$  increases

for small Curie temperatures,  $T_c^s \ll T_0$ . We now estimate the jump magnitude in Eq. (4): Using the realistic values:  $\Pi^2 = 0.3$ ,  $m_1^2 = 0.1$ ,  $\xi_0/a = 1$ ,  $T_0/T_c^s = 10$ , we obtain  $\Delta\rho/\rho \simeq 0.4$ , corresponding to a jump  $\gamma = 60\%$ , where  $\gamma$  is defined by  $\rho_{\text{SPM}} = (1 + \gamma) \rho_{\text{SFM}}$ . This estimate agrees with the plot in Fig. 2.

*Non-Ohmic regime.*— So far we discussed the Ohmic regime in the absence of an additional external electric field (or applied voltage) only. In the presence of an electric field  $E$ , the hopping conductivity in the paramagnetic state is  $\sigma \sim \exp[-r/\xi - e^2/(\kappa r T) + eEr/T]$ , [25], with the inelastic co-tunneling localization length  $\xi^{\text{in}} = a/\ln[E_c^0/g_t^0(T^2 + (eEa)^2)]$ , [15, 21]. For sufficiently high electric fields  $E > T/e\xi$  the tunneling term,  $\exp(-r/\xi)$ , in the conductivity is not important. As a result the optimal hopping distance  $r_{\text{opt}}(E) \sim \xi \sqrt{E_\xi/E}$ , with the characteristic electric field  $E_\xi = e/(\kappa \xi^2)$ , and the resistivity  $\rho \sim \exp[r_{\text{opt}}(E)/\xi]$  are temperature independent.

Including the magnetization dependent tunneling conductance  $g_t(m^2)$  in the above consideration, one finds that the conductivity in the SPM state in the presence of a strong electric field  $\sigma(E, m^2)$  is given by Eq. (3) with  $T_0(m^2) \rightarrow \mathcal{E}_0(m^2)$  and  $T \rightarrow E$ , where  $\mathcal{E}_0(m^2) = E_0[1 - (2\xi_0/a) \ln(1 + \Pi^2 m^2)]$  is the characteristic electric field,  $E_0 = T_0/e\xi_0$ , and  $\xi_0 = a/\ln[E_c^0/([eaE]^2 g_t^0)]$ . Equation (3) with the above substitutions holds for electric fields  $T/[e\xi(m^2)] < E < \mathcal{E}_0(m^2)$ . The last inequality means that the optimal hopping length  $r_{\text{opt}}(E)$  is larger than the size of a single grain,  $a$ , while the first inequality ensures that the electric field  $E$  is still strong enough to cause non-Ohmic behavior. Using typical values [2] for  $a \approx 10\text{nm}$ ,  $T_0 \approx 10^3\text{K}$ ,  $\kappa \approx 3$ , and temperature  $T \approx 10^2\text{K}$  we estimate the window for electric fields as  $10^3\text{V/cm} < E < 10^5\text{V/cm}$ . The resistance ratio  $\Delta\rho/\rho$  in the presence of a strong electric field is still given by Eq. (4) with the substitution  $T_0(m_1^2) \rightarrow \mathcal{E}_0(m_1^2)$ . For small polarizations,  $\Pi^2 \ll 1$ , one obtains  $\Delta\rho/\rho \simeq (\xi_0/a) \sqrt{E_0/(T_c^s/e\xi_0)} \Pi^2 (1 - m_1^2)$ .

*Discussion.*— Past experimental studies of self-assembled ferromagnetic arrays were dealing either with their thermodynamic properties [1, 2, 3, 4], or with domain wall motion [26]. Investigations of the electronic transport and magnetoresistance (MR) were mostly restricted to the SPM state [27, 28], where variable range hopping was observed. The crossover region near  $T_c^s$  was only studied by numerical methods in the context of manganite systems [5, 9, 10]. The resistivity dependence below the Curie temperature  $T_c^s$  presented in Fig. 2 is different from the schematic behavior shown in Fig. 1 reflecting the experimental data on manganite systems of Ref. [12]. In these materials the resistance in the SFM state (below  $T_c^s$ ) is close to the quantum resistance [17] and therefore weakly depends on temperature. In our consideration we assumed, based on the experiments [1, 3, 13, 16], that in the SFM state the sample resistance is much larger than the quantum resistance [17], meaning that it ex-



hibits variable range hopping behavior and therefore is more sensitive to temperature than the resistance of manganite systems.

Recently the nanoscale granularity in manganese oxides was directly observed experimentally in  $\text{La}_{2-2x}\text{Sr}_{1+2x}\text{Mn}_2\text{O}_7$ , [29]. The cluster structure in these perovskite materials is introduced by dopants, creating the individual weakly coupled nanodomains. To describe the MR in these materials one has to take into account electron localization within each cluster. This means that besides the tunneling conductance,  $g_t$ , a finite grain conductance  $g_0$  has to be considered as well. In this case the total conductance can be written in the form  $g(T, m^2) = g_0(T) g_t(m^2) / [g_0(T) + g_t(m^2)]$ . Below the Curie temperature  $T_c^s$ , the tunneling conductance is small,  $g_t(1) \ll g_0(T < T_c^s)$ , such that  $g(T < T_c^s, 1) = g_t(1)$ , whereas above  $T_c^s$ , the grain conductance  $g_0(T)$  becomes small due to localization effects (e.g. Jahn-Teller effect [30]), leading to the formation of an insulation state, see e.g. [12]. In our paper we were assuming that  $g_0 \gg g_t$  therefore the localization effects within each grain are small. This situation is realized in e.g.  $\text{La}_{1-x}\text{A}_x\text{MnO}_3$  ( $A = \text{Sr}, \text{Ca}$ ), [31].

The above considerations were carried out at zero external magnetic field  $B$ . A finite field in ferromagnetic domain materials affects the SFM-SPM transition and leads to a reduction of the peak in the MR accompanied by a shift to higher temperatures with increasing  $B$ , which is parallel to the magnetization of the SFM at low  $T$  [Fig. 1 (bottom); Refs. [3, 12]]. This means that the distribution function  $f(\theta)$  favors small angles near  $T_c^s$ , i.e. the drop in  $m^2$  is smeared out.

To summarize, we have investigated transport properties of ferromagnetic nanoparticle arrays and nanodomain materials in the limit of weak coupling between grains in the SPM and SFM states in both Ohmic and non-Ohmic regimes. We have described the electron transport near the Curie temperature  $T_c^s$  in the artificially self-assembled superspin arrays and discussed possible applications of our results to a certain class of doped manganites, where localization effects within the clusters can be neglected. We derived the magnitude of the jump in the resistivity at the transition between the SPM and SFM states. We also discussed the influence of the magnetic field on the jump amplitude and the relation of our results to available experimental data.

**Acknowledgements.**— We thank Ken Gray, John Mitchell, Philippe Guyot-Sionnest, Heinrich Jaeger, Wai Kwok, and Xiao-Min Lin for useful discussions. This work was supported by the U.S. Department of Energy Office of Science through contract No. DE-AC02-06CH11357. A. G. acknowledges support by the DFG through a research grant. I. B. was supported by the UC-ANL Consortium for Nanoscience research.

- [2] C. T. Black *et al.*, Science **290**, 1131 (2000).
- [3] H. Zeng *et al.*, Phys. Rev. B **73**, 020402(R) (2006).
- [4] Y. Ding and S. A. Majetich, Appl. Phys. Lett. **87**, 022508 (2005); P. Poddar *et al.*, Phys. Rev. B **68**, 214409 (2003).
- [5] E. Dagotto *et al.*, Phys. Rep. **344**, 1 (2001).
- [6] N. Mathur and P. Littlewood, Phys. Today, **56** (1), 26 (2003).
- [7] S. Yunoki *et al.*, Phys. Rev. Lett. **80**, 845 (1998); A. Moreo *et al.*, Science **283**, 2034 (1999).
- [8] M. Fäth *et al.*, Science **285**, 1540 (1999).
- [9] M. Mayr *et al.*, Phys. Rev. Lett. **86**, 135 (2001).
- [10] A. Moreo *et al.*, Phys. Rev. Lett. **84**, 5568 (2000).
- [11] In this paper (i) the grains are mesoscopically different in the sense of disorder and their surface roughness on the atomic scale and (ii) the tunneling conductances are of the same order.
- [12] Y. D. Chuang *et al.*, Science **292**, 1509 (2001); Y. Moritomo *et al.*, Nature **380**, 141 (1996).
- [13] M. Uehara *et al.*, Nature **399**, 560 (1999).
- [14] For a Curie temperature  $T_c^s \sim 100\text{K}$  and dielectric constant  $\kappa \sim 3$  the critical grain size is  $a_c \sim 50\text{nm}$ . The mean energy level spacing  $\delta$  for a single cluster is expressed in terms of its volume  $V$  and the DOS  $\nu$  at the Fermi surface as  $\delta = (\nu V)^{-1}$ . In this paper we assume  $T_c^s \gg \delta$ .
- [15] I. S. Beloborodov *et al.*, Rev. Mod. Phys. **79**, 469 (2007).
- [16] Y. Tokura *et al.*, J. Appl. Phys. **79**, 5288 (1996).
- [17] In references [2, 3] the sample resistance ( $> 10\text{M}\Omega$ ) well exceeds the quantum resistance  $[h/(2e^2) = 12.9\text{k}\Omega]$ .
- [18] J. Inoue and S. Maekawa, Phys. Rev. B **53**, R11927 (1996).
- [19] Tunneling conductance  $g_t^0$  between two clusters  $i$  and  $j$  is expressed in terms of the tunneling matrix  $t$  and DOS  $\nu$ :  $g_t^0 = \langle |t|^2 \rangle \nu_i \nu_j$ .  $\langle \dots \rangle$  stands for disorder average.
- [20] The total probability  $\tilde{P}(\theta_1, \dots, \theta_N)$  can be factorized as long as the Coulomb interaction is short ranged, see [15].
- [21] D. A. Averin and Yu. V. Nazarov, Phys. Rev. Lett. **65**, 2446 (1990).
- [22] The two probabilities,  $\mathcal{P}_i^{\text{el}}$  and  $\mathcal{P}_i^{\text{in}}$ , are of the same order for temperatures  $T \simeq \sqrt{E_c \delta}$ . For temperatures larger than that,  $\xi^{\text{in}} > \xi^{\text{el}}$ , therefore inelastic co-tunneling is the dominant transport mechanism.
- [23] N. F. Mott, *Metal-Insulator Transitions*, Taylor and Francis, 1990; N. F. Mott, Adv. Phys. **16**, 49 (1967).
- [24] B. I. Shklovskii and A. L. Efros, *Electronic properties of Doped Semiconductors*, Springer, New York, 1988; L. Efros and B. I. Shklovskii, J. Phys. C **8**, L49 (1975).
- [25] B. I. Shklovskii, Fiz. Tekh. Poluprovodn. (S.-Petersburg) **6**, 2335 (1972) [Sov. Phys. Semicond. **6**, 1964 (1973)].
- [26] O. Petravic, A. Glatz, and W. Kleemann, Phys. Rev. B **70**, 214432 (2004).
- [27] T. Zhu and Y. J. Wang, Phys. Rev. B **60**, 11918 (1999).
- [28] G.N. Kakazei *et al.*, J. Appl. Phys. **90**, 4044 (2001); S. Sankar *et al.*, Phys. Rev. B **62**, 14273 (2000).
- [29] C.D. Ling *et al.*, Phys. Rev. B **62**, 15096 (2000). In this paper the compound  $\text{La}_{2-2x}\text{Sr}_{1+2x}\text{Mn}_2\text{O}_7$  was studied, with doping level  $x \in [0, 1]$ . For  $0.3 \lesssim x \lesssim 0.4$  this manganese oxide system has a SFM to SPM transition.
- [30] A. J. Millis *et al.*, Phys. Rev. Lett. **74**, 5144 (1995).
- [31] K. H. Kim *et al.*, Phys. Rev. B **55**, 4023 (1997).